Original Investigation

Conventional MRI Features of Central Nervous System Embryonal Tumor, Not Otherwise Specified in Adults: Comparison with Glioblastoma

Xiang Xiao, MD[1], Xian Liu, MD[1], Wen Liang, MD, Li-Ying Han, MM, Xiao-Dan Li, MM, Liu-Ji Guo, MM, Wen-Le He, MM, Xiao-Min Liu, MM, Jun Zhou, MD, Qiang Cai, MD, Yi-Kai Xu, MD, Xiang-Liang Tan, MD, Yuan-Kui Wu, MD

Rationale and Objectives: The purpose of this study was to explore conventional MRI features that can accurately differentiate central nervous system embryonal tumor, not otherwise specified (CNS ETNOS) from glioblastoma (GBM) in adults.

Materials and Methods: Preoperative conventional MRI images of 30 CNS ETNOS and 98 GBMs were analyzed by neuroradiologists retrospectively to identify valuable MRI features. Five blinded neuroradiologists independently reviewed all these MRI images, and scored MRI features on a five-point scale. Kendall's coefficient of concordance was used to measure inter-rater agreement. Diagnostic value was assessed by the area under the curve (AUC) of receiver operating curve, and sensitivity and specificity were also calculated.

Results: Seven MRI features, including isointensity on T1WI, T2WI, and FLAIR, ill-defined margin, severe peritumoral edema, ring enhancement, and broad-based attachment sign, were helpful for the differential diagnosis of these two entities. Among these features, ring enhancement showed the highest inter-rater concordance (0.80). Ring enhancement showed the highest AUC value (0.79), followed by severe peritumoral edema (0.67). The combination of seven features showed the highest AUC value (0.86), followed by that of three features (ill-defined margin, severe peritumoral edema, and ring enhancement) (0.83).

Conclusion: Enhancement pattern, peritumoral edema, and margin are valuable for the discrimination between CNS ETNOS and GBM in adults.

Key Words: Embryonal tumor; Glioma; Magnetic resonance imaging; Diagnostic imaging; ROC curve.

© 2021 The Association of University Radiologists. Published by Elsevier Inc. All rights reserved.

INTRODUCTION

Central nervous system embryonal tumor, not otherwise specified (CNS ETNOS) is a new naming based on the 2016 WHO classification of tumors of the CNS (1). It is composed of poorly differentiated neuroepithelial cells with the potential of multilineage differentiation, without molecular genetic variation characteristics of other CNS tumors (2,3). One of the outstanding features of the malignant character of CNS ETNOS is its high propensity to remote dissemination via the cerebrospinal fluid (CSF) pathways and even systemic dissemination, such as to the lungs, livers, bone marrow, and lymph nodes (4). Clinically, an MRI examination of the spinal canal and examination of CSF cytology should be performed when a CNS ETNOS tumor is suspected (5–7). Moreover, postoperative radiotherapy should include the entire neuroaxis for the prevention of spinal seeding (8). Also, aggressive chemotherapy such as intrathecal chemotherapy following radical resection is recommended (7,9). Unfortunately, the prognosis for CNS ETNOS is generally poor, and overall survival rarely extends beyond 24 months in spite of therapy with surgery, radiotherapy and chemotherapy (8). Therefore, accurate preoperative identification of CNS ETNOS has important implications for patient management and treatment planning (9,10).

MRI is the preferred technique for the evaluation of intracranial tumors. However, it is very difficult to accurately

Acad Radiol 2021; ■:1–8

From the Department of Medical Imaging, Nanfang Hospital, Southern Medical University, No. 1838 Guangzhou Avenue North, Guangzhou, Guangdong 510515, China (X.X., X.-D.L., L.-J.G., W.-L.H., X.-M.L., Y.-K.X., X.-L.T., Y.-K.W.); Department of Radiology, Guangdong Provincial Hospital of Traditional Chinese Medicine, Guangzhou, China (X.L.); Department of Radiology, Zhujiang Hospital, Southern Medical University, Guangzhou, China (W.L., L.-Y.H.); Department of Pathology, Nanfang Hospital, Southern Medical University, Guangzhou, China (J.Z.); Okra Medical Technology Co., Ltd., Suzhou, China (Q.C.). Received August 8, 2020; revised January 6, 2021; accepted January 8, 2021. **Address correspondence to:** Y.-K.W. e-mail: ripleyor@126.com

[1] Xiang Xiao and Xian Liu have contributed equally to this work.

© 2021 The Association of University Radiologists. Published by Elsevier Inc. All rights reserved.

https://doi.org/10.1016/j.acra.2021.01.010

differentiate CNS ETNOS from glioblastoma (GBM) using biomarkers derived from functional MRI. Both tumors are hypercellular histologically and demonstrate limited diffusion on DWI images (11,12). Also, both of them have rich blood supply and increased vascular permeability, leading to similar rCBV values measured on dynamic susceptibility contrast perfusion weighted imaging (DSC-PWI) and K^{trans} values on dynamic contrast enhancement perfusion weighted imaging (13). Furthermore, as shown in a study with MR spectroscopy, neither choline nor N-acetyl-aspartate concentration could make the distinction between them (14). A few researchers claimed that the Taurine concentration was a useful discriminator between CNS ETNOS and GBM (15,16). However, this metabolite is not commonly used and the related post-processing is complex, which greatly hinders its clinical application. Interestingly, compared with these functional MRI techniques, conventional MRI seems to be more valuable in the differential diagnosis between these two types of tumors. Some MRI features have been reported to be characteristic for them, such as signal intensity of T1WI, T2WI and FLAIR, border and peritumoral edema (7,13,17,18). However, all these signs are prone to subjectivity and inter-observer variability. To the best of our knowledge, the diagnostic values of these conventional MRI features have not been systematically analyzed.

The present study investigated the diagnostic value of all of these features individually or in combinations for differentiation between CNS ETNOS and GBM through the receiver operating curve (ROC) analysis.

MATERIALS AND METHODS

Patients

The study was approved by the institutional research ethics committee of Nanfang Hospital, Southern Medical University, and the written informed consent was waived due to the retrospective nature of our study. We used the picture archiving and communication system (PACS) program to search our radiology database from January 2011 to December 2019 to obtain MRI data of CNS ETNOS and GBMs. Thirty one patients with ETNOS and the first 100 consecutive patients with GBM were enrolled into the study according to the following including criteria: (1) available pretreatment brain MRI; (2) final diagnosis confirmed by surgery and histopathologic examinations. The diagnosis of all these tumors was established based on the 2016 WHO classification of tumors of the CNS. Three cases were excluded for motion artifacts. Eventually, 128 cases of tumors were included in this study, including 30 cases of CNS ETNOS (16 females; age range 19−69 years; average age 40.00 ± 14.17 years) and 98 cases of GBMs (38 females; age range 21−78 years; average age 52.80 ± 14.13 years).

MRI Parameters

Patients were examined on 3.0T MRI scanners (Signa Excite, GE, USA; Achieva, Philips, The Netherlands) with the use of a head coil. All of the 128 patients underwent MRI protocols comprised of axial T1WI, T2WI, FLAIR, DWI and axial, sagittal and coronal contrast-enhanced T1WI. The imaging parameters are summarized in supplementary materials (see Supplementary Table 1). For all patients, contrast agent (Omniscan TM, GE Healthcare, Ireland; Gadopentetate dimeglumine, Consun, Guangzhou, China) was intravenously bolus injected via a power injector with a flow rate of 2.0−2.5 mL/s at a dose of 0.2 mmol/kg of body weight, followed by a 20 mL bolus of saline with the same injection rate. The clinical data, including demographic information, duration of symptoms, cerebrospinal fluid dissemination, treatment, follow-up time, and prognosis, were recorded and evaluated.

Image Analysis

The conventional MRI features, including location (cortex and subcortex, deep white matter), margin (well-defined, ill-defined), T1WI, T2WI, FLAIR and DWI signal relative to the gray matter (hypointensity, isointensity, hyperintensity), enhancement pattern (ring enhancement, other enhancement patterns), cystic change or necrosis, flow void sign, intratumoral hemorrhage, broad-based attachment sign, peritumoral edema (mild or moderate, severe) and tumor volume, were evaluated and compiled by two radiologists (Xiang Xiao and Xian Liu, with 5 and 10 years of experience, respectively) in a blind manner. Discrepancies were resolved in consensus during a joint evaluation with a third radiologist (Yuan-Kui Wu, with 20 years of experience). Another expert radiologist (Xiang-Liang Tan, with 15 years of experience) diagnosed all cases as CNS ETNOS or GBM in a blinded way.

These MRI features showing significant difference between CNS ETNOS and GBM were introduced to five radiologists (Li-Ying Han, Liu-Ji Guo, and Xiao-Min Liu, each with 5 years of experience; Xiao-Dan Li, with 8 years of experience; Wen-Le He, with 10 years of experience). These radiologists, blinded to histopathological diagnoses, independently recorded the confidence level of the presence of every single feature in each case of tumor using a 5-point scale: 1 = definitely not present; 2 = probably not present; 3 = equivocal; 4 = probably present; 5 = definitely present. The window width, window level and zoom of images were adjusted through the tools included in the PACS program as needed.

Statistical Analysis

First, continuous variables are presented as mean ± standard error, and differences between variables were analyzed using independent-samples *t* test. Differences in categorical variables were analyzed using the χ^2 or Fisher's exact tests, as appropriate. Second, Kendall's coefficient of concordance (W) was used to measure inter-rater agreement, with W ≥0.21 representing fair, W ≥0.41 moderate, W ≥0.61 substantial, and W ≥0.81 almost perfect concordances (19).

Third, ROC curve analysis was performed to assess the diagnostic performance of MRI feature individual or in combinations, as well as that of the expert radiologist, with CNS ETNOS cases scored as 1, while GBM cases were marked as 0 according to the gold standard served by pathological diagnosis. Areas under the curves (AUCs), sensitivities and specificities of each MRI feature were calculated. Fourth, four separate multivariate logistic regression analyses were conducted based on different predictor selection methods, including all MRI features, features with W $\geq$0.61, features with W $\geq$0.61 selected by forward method, and features justified by experts. All the statistical analyses above were performed using SPSS software (Version 20.0). Finally, the comparison between every two AUCs was made by the nonparametric approach of Delong & Clarke-Pearson conducted in MedCalc software (Version 15.2.2). The Benjamini-Hochberg method was used to control the false discovery rate (FDR) of multiple comparisons. The difference was considered statistically significant if $p < 0.05$.

RESULTS

Clinical Features

The clinical characteristics of CNS ETNOS and GBM are summarized in Table 1. CNS ETNOS patients had more cerebrospinal fluid dissemination than did GBM patients ($p< 0.05$). The overall survival time of CNS ETNOS was much shorter than that of GBM ($p< 0.05$).

Conventional MRI Features

MRI findings of CNS ETNOS and GBM are summarized in Table 2. Seven MRI features were significantly different between the two groups ($p < 0.05$). DWI did not have enough power for the discrimination between them. Generally, GBM showed ill-defined margin, severe peritumoral edema, and ring enhancement. In contrast, CNS ETNOS showed well-defined border, minimal peritumoral edema and isointensity on T1WI, T2WI and FLAIR, as well as broad-based attachment sign. Representative cases of the MRI features, which contributed greatly to the accurate differential diagnosis between GBM and CNS ETNOS, are shown in Figures 1–3.

Inter-rater Agreement for Each MRI Feature

Supplemental Table 2 summarizes the W values of these seven MRI features. Ring enhancement showed the highest inter-rater concordance (0.80), with the same level of concordance as ill-defined margin (0.70), severe peritumoral edema (0.76), and broad-based attachment sign (0.67). A moderate inter-rater agreement was recorded for isointensity on T1WI (0.55), T2WI (0.55), and FLAIR (0.59).

Diagnostic Performance of the MRI Features Individually or in Combination

The AUC values of these seven features were all above 0.5, with ring enhancement being the highest (0.79), followed by severe peritumoral edema (0.67) (Table 3, Fig 4a; the results of all ratings are shown in Supplementary Table 3). Ring enhancement also presented the maximum sensitivity (74%), followed by severe peritumoral edema (61%). Isointensity on T1WI had the highest specificity (82%), followed by ring enhancement (75%).

TABLE 1. Clinical Findings of CNS ETNOS and GBM

Variable	CNS ETNOS (30)		GBM (98)		*p* Value
	No.	%	No.	%	
Sex					
Female	16	53.3	38	38.8	0.158
Male	14	46.7	60	61.2	
Age (Y)	40.00 ± 14.17 (19 ~ 69)		52.80 ± 14.13 (21 ~ 78)		0.001
Onset time (M)	1.20 ± 1.18 (0.03–4)		1.50 ± 1.44 (0.03–6)		0.530
CSF dissemination	5	16.7	0	0	0.001
Treatment					
Resection	30	100	96	98	1
Radiotherapy	30	100	93	94.9	0.590
Chemotherapy	29	96.7	95	96.9	1
Follow-up time (M)	15.30 ± 10.96 (3–36)		17.86 ± 12.55 (4–48)		0.317
Outcome					
Recurrence	20	66.7	63	64.3	0.811
PFS (M)	6.45 ± 2.80 (2–11)		7.94 ± 3.23 (3–15)		0.068
Death	24	80	77	78.6	0.867
OS (M)	10.13 ± 3.44 (3–16)		12.27 ± 4.76 (4–23)		0.019

CNS ETNOS, Central nervous system embryonal tumor, not otherwise specified; CSF, cerebrospinal fluid; GBM, glioblastoma; M, month; OS, overall survival; PFS, progression free survival; Y, year.

TABLE 2. MRI Findings of CNS ETNOS and GBM in Adults

MRI Findings	CNS ENOS (30)		GBM (98)		*p* Value
	No.	%	No.	%	
Location					
Cortex and subcortex	17	56.7	41	41.8	0.153
Deep white matter	13	43.3	57	58.2	
Margin					
Well-defined	22	73.3	26	26.5	0.000
Ill-defined	8	26.7	72	73.5	
T1WI					
Hypointensity	16	53.3	89	90.8	0.000
Isointensity	14	46.7	9	9.2	
T2WI					
Isointensity	12	40	5	5.1	0.000
Hyperintensity	18	60	93	94.9	
FLAIR					
Isointensity	18	60	6	6.1	0.000
Hyperintensity	12	40	92	93.9	
DWI					
Isointensity	2	6.7	3	3.1	0.334
Hyperintensity	28	93.3	95	96.9	
Enhancement					
Ring enhancement	7	23.3	68	69.4	0.000
Other enhancement patterns	23	76.7	30	30.6	
Cystic change or necrosis	24	80	87	88.8	0.228
Flow void sign	10	33.3	23	23.5	0. 280
Intratumoral hemorrhage	5	16.7	26	26.5	0. 270
Broad-based attachment sign	15	50	22	22.4	0.004
Peritumoral edema					
Mild or Moderate	24	80	35	35.7	0.000
Severe	6	20	63	64.3	
Tumor volume (cm^3)	106.66 ± 60.20		76.84 ± 80.11		0.197

CNS ETNOS, Central nervous system embryonal tumor, not otherwise specified; GBM, glioblastoma; MRI, magnetic resonance imaging.

Among different combinations of these MRI features, the combination of all features (Comb_7) showed the highest AUC value (0.86), followed by that of four features (Comb_4: ill-defined margin, severe peritumoral edema, ring enhancement and broad-based attachment sign, 0.83), that of three features (Comb_3: ill-defined margin, severe peritumoral edema and ring enhancement, 0.83) and that of two features (Comb_2: ill-defined margin and ring enhancement, 0.82) (Table 4, Fig 4b).

Comparison of the AUC values for all pairs is summarized in Supplemental Table 4. Comb_7 showed the best diagnostic performance ($p< 0.05$). Comb_4, Comb_3 and Comb_2 did not show significant difference between them but were higher than the expert radiologist ($p< 0.05$) and all single MRI features ($p< 0.05$). Ring enhancement showed the highest performance among all single MRI features ($p< 0.001$).

DISCUSSION

The accurate differential diagnosis between CNS ETNOS and GBM in adults is of great importance clinically. The present study found that CNS ETNOS differed from GBM in terms of the enhancement pattern, peritumoral edema, border, broad-based attachment sign, and signal intensities on conventional MRI images.

Many scholars attempted to explore the specific pattern of enhancement for CNS ETNOS (7,20,21), and claimed that both GBMs and CNS ETNOS showed inhomogeneous marked enhancement. Indeed, the majority cases of CNS ETNOS in our study presented heterogeneous significant enhancement, which was consistent with the identity of highly malignant tumor. However, researchers seemed to have ignored the fact that ring enhancement is a common sign for GBMs. We rarely encounter with CNS ETNOS showing ring enhancement in our clinical practice. In the present study, this sign showed the highest inter-rater concordance, AUC value, and sensitivity among all seven conventional MRI features. Also, its specificity was second only to that of isointensity on T1WI. Given the low inter-rater concordance of isointensity on T1WI, ring enhancement sign should be the most valuable feature for the differential diagnosis between them. Nevertheless, the exact pathological mechanism of this phenomenon is not clear yet. In our opinion, this is likely because CNS ETNOS is readily closer to the surface of the cerebrum and thus may have richer blood supply, in contrast to GBM that commonly originates from deep white matter (22). However, both tumors showed similar hemodynamic characteristics such as blood vessel leakiness and blood volume (13). Therefore, the homeostasis of the microvasculature of these two types of tumors needs to be further investigated (23).

Many studies showed that CNS ETNOS tends to have a clear boundary (7,13,14,20,21,24). In contrast, GBMs nearly always show ill-defined borders (17). It was reported that the tumor cells of CNS ETNOS generally demonstrate an expansive pattern of growth (13). In contrast, GBMs are biologically characterized by an invasive growth along the white-matter tracts and perivascular space (25). However, the inter-rater concordance and AUC value of the sign of ill-defined margin were lower than we had anticipated. This may be explained by the fact that CNS ETNOS tends to show similar intensities to gray matter and invade cortex and subcortical regions, which would have affected the evaluation of the border between the tumor and its surroundings in the study. Therefore, redefinition of this sign might improve the diagnostic performance, which needs to be clarified in future studies.

CNS ETNOS often shows no or mild peritumoral edema (13,20,21,24). In contrast, GBM is often associated with severe peritumoral edema (18). In the present study, severe peritumoral edema exhibited the second highest inter-rater concordance and AUC value. It should be noted that the degree of peritumoral edema can be quantified as mild, moderate and severe using certain criteria (26). Whereas, it is

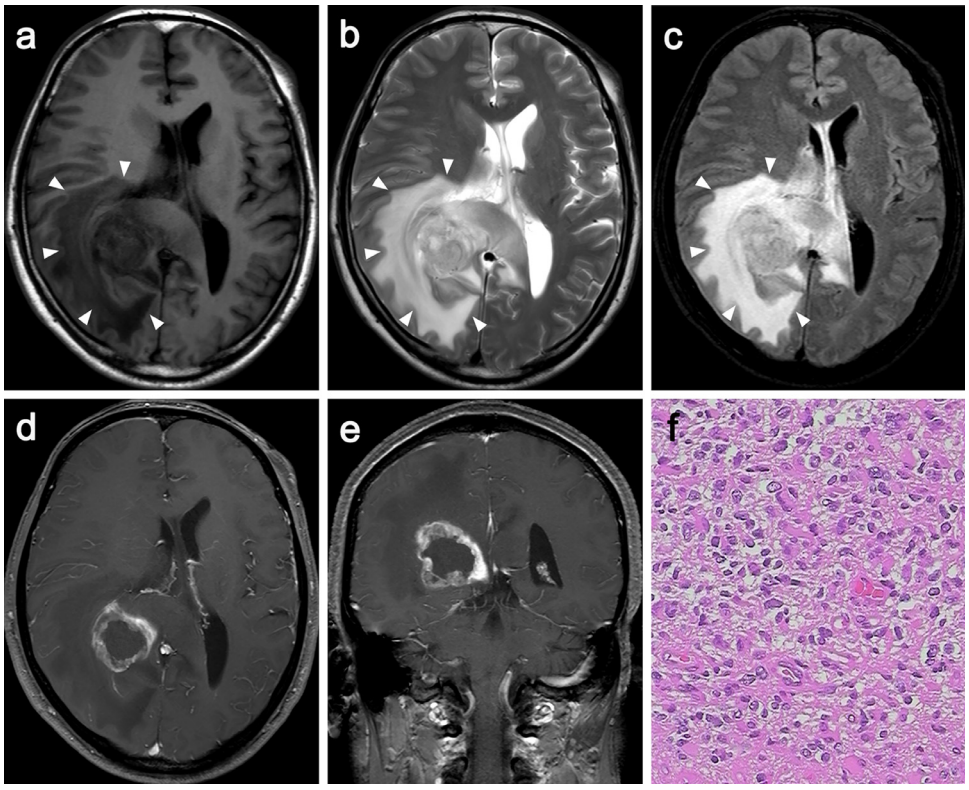

Figure 1. Representative case of GBM. A 57-year-old man with GBM in the right parietal lobe. The tumor shows ill-defined border and severe peritumoral edema (arrowheads) on axial T1WI (a), T2WI (b) and FLAIR (c) images, and ring enhancement on axial (d) and coronal (e) contrast-enhanced T1-weighted images. Hematoxylin-Eosin staining showing mitotic figures (f, × 200). GBM, glioblastoma.

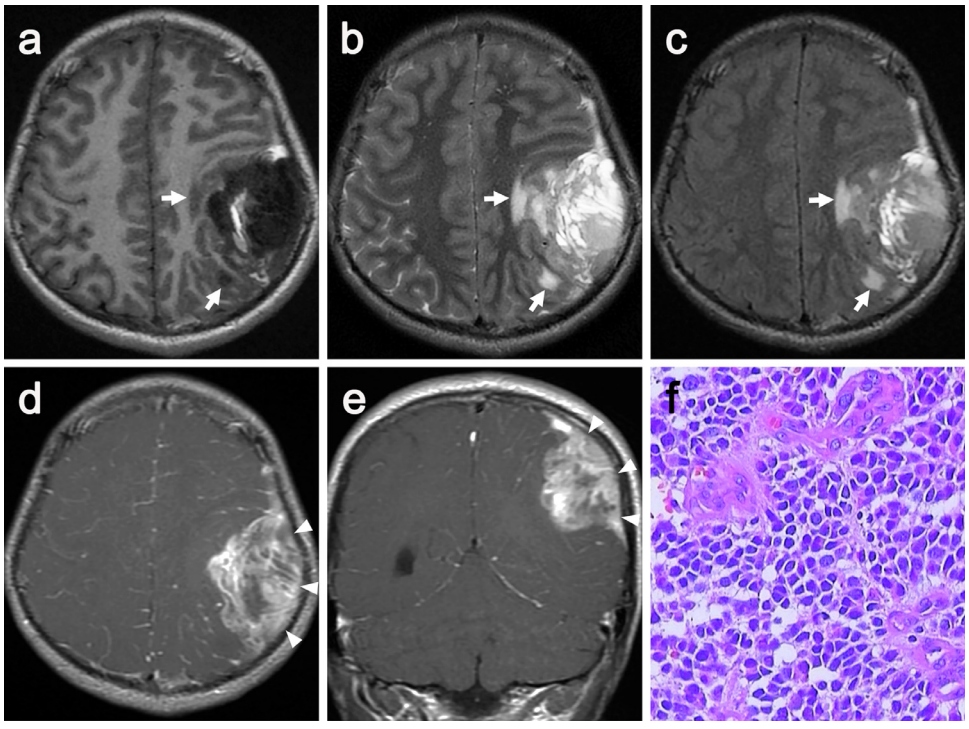

Figure 2. Representative case of CNS ETNOS. A 36-year-old man with CNS ETNOS in the left parietal lobe. The tumor shows well-defined border, cystic changes, necrosis, hemorrhage and mild peritumoral edema (arrows) on axial T1WI (a), T2WI (b) and FLAIR (c) images, and shows inhomogeneous, marked enhancement and broad-based attachment sign (arrowheads) on axial (d) and coronal (e) contrast-enhanced T1-weighted images. Hematoxylin-Eosin staining showing Homer-Wright pseudorosettes structure (f, × 200). CNS ETNOS, Central nervous system embryonal tumor, not otherwise specified.

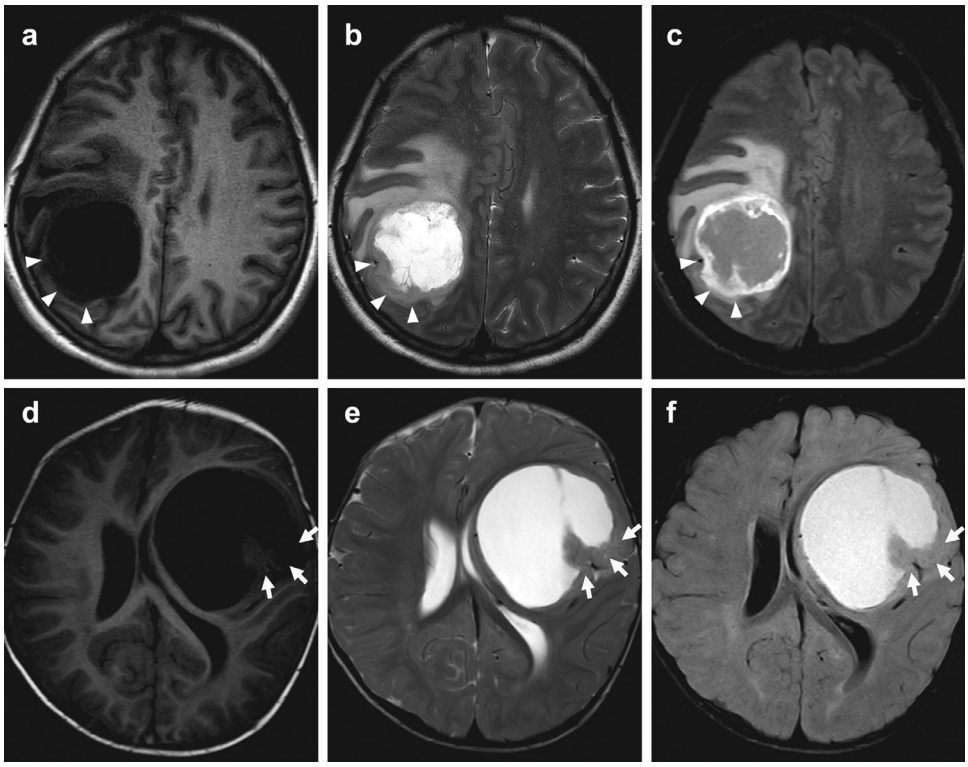

Figure 3. Comparison of T1WI, T2WI and FLAIR signal of GBM and CNS ETNOS. (a-c) A 58-year-old woman with GBM in the right parietal lobe. The solid part (arrowheads) of the tumor shows hypointensity on axial T1WI (a) images and hyperintensity on axial T2WI (b) and FLAIR (c) images. (d-f) A 19-year-old woman with ETNOS in the left frontotemporal lobe. The solid part (arrows) of the tumor shows isointensity on axial T1WI (d), T2WI (e), and FLAIR (f) images. CNS ETNOS, Central nervous system embryonal tumor, not otherwise specified; GBM, glioblastoma.

TABLE 3. AUC, Sensitivity and Specificity of Seven MRI Features for Differentiation Between CNS ETNOS and GBM in Adults

Sign		Observer					Mean
		1	2	3	4	5	
Isointensity on T1WI	AUC	0.57	0.56	0.66	0.64	0.59	0.58
	Sensitivity	45%	25%	45%	80%	45%	33%
	Specificity	74%	86%	88%	44%	73%	82%
Isointensity on T2WI	AUC	0.62	0.54	0.75	0.63	0.60	0.61
	Sensitivity	35%	65%	75%	75%	65%	57%
	Specificity	86%	50%	72%	44%	54%	61%
Isointensity on FLAIR	AUC	0.61	0.51	0.64	0.64	0.63	0.60
	Sensitivity	75%	95%	55%	80%	60%	56%
	Specificity	42%	9%	74%	44%	63%	63%
Ill-defined margin	AUC	0.61	0.68	0.64	0.57	0.62	0.62
	Sensitivity	55%	90%	40%	85%	65%	55%
	Specificity	62%	45%	92%	27%	54%	61%
Severe peritumoral edema	AUC	0.69	0.73	0.73	0.60	0.69	0.67
	Sensitivity	80%	65%	65%	35%	60%	61%
	Specificity	54%	77%	79%	85%	70%	70%
Ring enhancement	AUC	0.81	0.80	0.86	0.80	0.75	0.79
	Sensitivity	90%	85%	100%	75%	55%	74%
	Specificity	63%	64%	64%	83%	90%	75%
Broad-based attachment sign	AUC	0.56	0.53	0.57	0.53	0.54	0.55
	Sensitivity	25%	70%	65%	75%	20%	53%
	Specificity	95%	38%	55%	39%	89%	57%

AUC, area under the curve; CNS ETNOS, Central nervous system embryonal tumor, not otherwise specified; GBM, glioblastoma; MRI, magnetic resonance imaging.

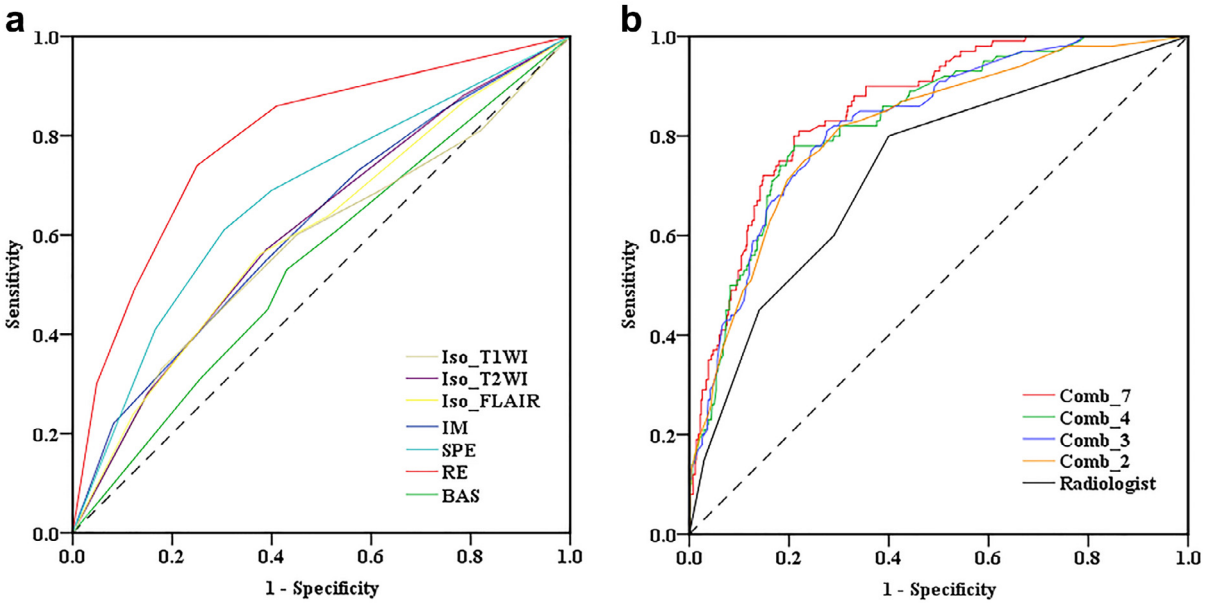

Figure 4. Composite ROC curves of conventional MRI features. a, ROC curves of seven individual MRI features. Ring enhancement shows the highest AUC (0.79), followed by severe peritumoral edema (0.67). Isointensity on T2WI, isointensity on FLAIR, and ill-defined margin exhibit similar AUC values, which are larger than those of isointensity on T1WI and broad-based attachment sign. b, ROC curves of MRI features in combinations. The combination of seven features shows the highest AUC value (0.86). The combinations of four features, three features and two features exhibit similar AUC values (0.83, 0.83, and 0.82, respectively). The radiologist shows the lowest AUC value (0.73). Iso_T1WI, isointensity on T1WI; Iso_T2WI, isointensity on T2WI; Iso_FLAIR, isointensity on FLAIR; IM, ill-defined margin; SPE, severe peritumoral edema; RE, ring enhancement; BAS, broad-based attachment sign; Comb_7, combination of seven features; Comb_4, combination of ill-defined margin, severe peritumoral edema, ring enhancement and broad-based attachment sign; Comb_3, combination of ill-defined margin, severe peritumoral edema and ring enhancement; Comb_2, combination of ill-defined margin and ring enhancement. AUC, area under the curve; MRI, magnetic resonance imaging; ROC, receiver operating curve.

rather common to subjectively assess the degree of peritumoral edema in clinical practice. We evaluated the presence of severe peritumoral edema based on a five-point scale in order to be in line with other MRI features addressed in the present study.

The broad-based attachment sign showed a low sensitivity and specificity in this study. In general, GBM has a lower chance to develop this sign owing to its origin in deep white matter. Whereas, 33 cases of GBMs in this study were very large, with a diameter >5.0 cm, and abutted on the brain surface. On the other hand, 13 cases of CNS ETNOS were located near the midline and thus did not present with the broad-based attachment sign (20,27). However, among the remaining 17 cases of CNS ETNOS located in the superficial regions of the brain, 15 cases (88.2%) showed this sign.

According to previously published reports, CNS ETNOS are usually isointense to gray matter on T1WI, T2WI, and FLAIR (12,13,24), probably due to the high nucleus-to-cytoplasm ratio and less interstitial water (13,24). In contrast, GBMs often show hypointensity on T1WI and hyperintensity on T2WI and FLAIR. However, these three features showed poor diagnostic performance in discriminating CNS ETNOS from GBM in this present cohort. Moreover, the inter-rater agreements of them were lower than those of other MRI features. The reason may be that CNS ETNOS is prone to cystic degeneration, necrosis, and hemorrhage

TABLE 4. AUC, Sensitivity and Specificity of Different MRI Features Combinations for Differentiation Between CNS ETNOS and GBM in Adults

Features Combination	AUC	SE	*p*Value	Youden Index	Sensitivity	Specificity
Comb_7	0.86	0.018	<0.001	0.590	80%	79%
Comb_4	0.83	0.021	<0.001	0.570	78%	79%
Comb_3	0.83	0.022	<0.001	0.534	81%	73%
Comb_2	0.82	0.023	<0.001	0.520	75%	77%

Comb_7, combination of seven features; Comb_4, combination of ill-defined margin, severe peritumoral edema, ring enhancement and broad-based attachment sign; Comb_3, combination of ill-defined margin, severe peritumoral edema and ring enhancement; Comb_2, combination of ill-defined margin and ring enhancement. AUC, area under the curve; CNS ETNOS, Central nervous system embryonal tumor, not otherwise specified; GBM, glioblastoma; MRI, magnetic resonance imaging.

(7,8,11,21,24,28) and the resultant mixed signals within the tumor might have significantly confounded the evaluation.

The combinations of these conventional MRI features significantly improved the diagnostic performance in this study. However, although the AUC of the combination of seven MRI features was higher than any of other combinations, the benefit was relatively little and at the cost of significantly increased workload. In contrast, the combinations of two (ill-defined margin and ring enhancement), three (ill-defined margin, severe peritumoral edema, and ring enhancement) and four features (ill-defined margin, severe peritumoral edema, ring enhancement, and broad-based attachment sign) seems to be more practicable in clinical practice.

Our study has several limitations. First, the sample sizes of these two tumors were unbalanced due to the rarity of CNS ETNOS. However, the ROC plot provides a global comprehensive view of the test, and the AUC value is independent of the prevalence (29). Second, functional MRI such as MRS and DSC-PWI were not involved in this study, due to the low value in differential diagnosis. Third, no neurosurgeons participated in the study. Last but not the least, it was a retrospective study. Further prospective studies are warranted to validate these observations in this study.

CONCLUSION

In this largest MRI cohort on differential diagnosis between CNS ETNOS and GBM in adults to date, seven conventional MRI features showed practical and positive ability for differentiation. CNS ETNOS can be accurately differentiated from GBM by evaluating the margin, peritumoral edema and enhancement pattern.

REFERENCES

1. Louis DN, Perry A, Reifenberger G, et al. The 2016 world health organization classification of tumors of the central nervous system: a summary. Acta Neuropathol 2016; 131:803–820.
2. Visee S, Soltner C, Rialland X, et al. Supratentorial primitive neuroectodermal tumours of the brain: multidirectional differentiation does not influence prognosis. A clinicopathological report of 18 patients. Histopathology 2005; 46:403–412.
3. Pickles JC, Hawkins C, Pietsch T. CNS embryonal tumours: WHO 2016 and beyond. Neuropath Appl Neuro 2018; 44:151–162.
4. Becker LE, Hinton D. Primitive neuroectodermal tumors of the central nervous system. Hum Pathol 1983; 14:538–550.
5. Tomita T, McLone D, Yasue M. Cerebral primitive neuroectodermal tumors in childhood. J Neurooncol 1988; 6:233–243.
6. Wang KC, Chi Je G, Cho BK. Biological behavior of the primitive neuroectodermal tumor. Seoul J Med 1988; 29:293–303.
7. Pickuth D, Leutloff U. Computed tomography and magnetic resonance imaging findings in primitive neuroectodermal tumours in adults. Brit J Radiol 1996; 69:1–5.
8. Kouyialis AT, Boviatsis EI, Karampelas IK, et al. Primitive supratentorial neuroectodermal tumor in an adult. J Clin Neurosci 2005; 12:492–495.
9. Yang HJ, Nam DH, Wang KC, et al. Supratentorial primitive neuroectodermal tumor in children: clinical features, treatment outcome and prognostic factors. Child Nerv Syst 1999; 15:377–383.
10. Burger PC. Supratentorial primitive neuroectodermal tumor (sPNET). Brain Pathol 2006; 6:86.
11. Klisch J, Husstedt H, Hennings S, et al. Supratentorial primitive neuroectodermal tumours: diffusion-weighted MRI. Neuroradiology 2000; 42:393–398.
12. Erdem E, Zimmerman RA, Haselgrove JC, et al. Diffusion-weighted imaging and fluid attenuated inversion recovery imaging in the evaluation of primitive neuroectodermal tumors. Neuroradiology 2001; 43:927–933.
13. Law M, Kazmi K, Wetzel S, et al. Dynamic susceptibility contrast-enhanced perfusion and conventional MR imaging findings for adult patients with cerebral primitive neuroectodermal tumors. Am J Neuroradiol 2004; 25:997–1005.
14. Kim DG, Lee DY, Paek SH, et al. Supratentorial primitive neuroectodermal tumors in adults. J Neuro-Oncol 2002; 60:43–52.
15. Majos C, Alonso J, Aguilera C, et al. Adult primitive neuroectodermal tumor: proton MR spectroscopic findings with possible application for differential diagnosis. Radiology 2002; 225:556–566.
16. Kovanlikaya A, Panigrahy A, Krieger MD, et al. Untreated pediatric primitive neuroectodermal tumor in vivo: quantitation of taurine with MR spectroscopy. Radiology 2005; 236:1020–1025.
17. Upadhyay N, Waldman AD. Conventional MRI evaluation of gliomas. Brit J Radiol 2011; 84:S107–S111.
18. Asari S, Makabe T, Katayama S, et al. Assessment of the pathological grade of astrocytic gliomas using an MRI score. Neuroradiology 1994; 36:308–310.
19. Levitan B, Yee CL, Russo L, et al. A model for decision support in signal triage. Drug Saf 2008; 31:727–735.
20. Dai AI, Backstrom JW, Burger PC, et al. Supratentorial primitive neuroectodermal tumors of infancy: clinical and radiologic findings. Pediatric neurol 2003; 29:430–434.
21. Nowak J, Seidel C, Pietsch T, et al. Systematic comparison of MRI findings in pediatric ependymoblastoma with ependymoma and CNS primitive neuroectodermal tumor not otherwise specified. Neuro-Oncology 2015; 17:1157–1165.
22. Aronen HJ, Gazit IE, Louis DN, et al. Cerebral blood volume maps of gliomas: comparison with tumor grade and histologic findings. Radiology 1994; 191:41–51.
23. Hua J, Liu P, Kim T, et al. MRI techniques to measure arterial and venous cerebral blood volume. NeuroImage 2019; 187:17–31.
24. Chawla A, Emmanuel JV, Seow WT, et al. Paediatric PNET: pre-surgical MRI features. Clin Radiol 2007; 62:43–52.
25. Blasel S, Jurcoane A, Franz K, et al. Elevated peritumoural rCBV values as a mean to differentiate metastases from high-grade gliomas. Acta Neurochir 2010; 152:1893–1899.
26. Bradac GB, Ferszt R, Bender A, et al. Peritumoral edema in meningiomas. A radiological and histological study. Neuroradiology 1986; 28:304–312.
27. Barros Palau AE, Khan K, Morgan ML, et al. Suprasellar primitive neuroectodermal tumor in an adult. J Neuro-Ophthalmol 2016; 36:299–303.
28. Ohba S, Yoshida K, Hirose Y, et al. A supratentorial primitive neuroectodermal tumor in an adult: a case report and review of the literature. J Neuro-Oncol 2008; 86:217–224.
29. Zweig MH, Campbell G. Receiver-operating characteristic (ROC) plots: a fundamental evaluation tool in clinical medicine. Clin Chem 1993; 39:561–577.

SUPPLEMENTARY MATERIALS

Supplementary material associated with this article can be found in the online version at doi:10.1016/j.acra.2021.01.010.